AN ADAPTIVE REACHING LAW BASED THREE-DIMENSIONAL GUIDANCE LAWS FOR INTERCEPTING HYPERSONIC VEHICLE

Yujie Si[1], Shenmin Song[1] and Xiqing Wei[2]

[1]School of Astronautics
Harbin Institute of Technology
No. 92, West Dazhi Street, Nangang District, Harbin 150001, P. R. China
siyujiehit@126.com; songshenmin@hit.edu.cn

[2]Research and Development Department
Shanghai Electro-Mechanical Engineering Institute
No. 3888, Yuanjiang Road, Minhang District, Shanghai 200000, P. R. China
xiqingwei@126.com

ABSTRACT. *The interception of hypersonic vehicles is a formidable challenge due to its high speed and strong maneuverability; besides, traditional guidance methods cannot guarantee interception accuracy. To solve this problem, three-dimensional sliding mode guidance laws are proposed in this paper based on the head pursuit guidance method. The first guidance law ensures that the dynamic system converges to head pursuit guidance conditions in finite time without the knowledge of external disturbances, and can also weaken the chattering phenomenon. In practical application, the capacity of dynamic actuators is limited. Therefore, a guidance law with input saturation is proposed using the hyperbolic tangent function and auxiliary system. This method is novel in which the system can be ensured finite-time and asymptotically stable. In theory, the two guidance laws can be proved using Lyapunov stability theory. The correctness and effectiveness of the methods are verified by numerical simulations.*
Keywords: Three-dimensional guidance law, Hypersonic vehicle, Head pursuit, Sliding mode guidance law, Adaptive method

1. **Introduction.** The hypersonic cruise targets with the characteristics of high speed, strong maneuverability and good concealment are difficult to be intercepted. Currently, the interceptor no longer has an advantage in speed compared to the hypersonic vehicle target, and improving the speed of the interceptor imposes a great test not only for the technology but also for the economic test. To solve this problem, Golan and Shima [1] first proposed a head pursuit method for intercepting hypersonic vehicle in 2004. Using this method, the closing velocity becomes very low, which can greatly reduce the energy consumption of the interceptor. Another advantage is that the head pursuit guidance method can eliminate the perturbation of interceptor of detection induced by aerodynamic heating. In [1,2], the authors put forward the concepts and conditions of the head pursuit guidance. In addition, two-dimensional sliding mode guidance laws were proposed. In [3], a bang-bang controller was designed in two-dimensional engagement. In [4], a head pursuit guidance law considering the dynamic characteristics of the system was proposed in two-dimensional engagement, but this guidance law cannot deal with the external disturbance. A three-dimensional variable structure guidance law was proposed based on the head pursuit guidance method in [5], but the upper bound of the external disturbance was still assumed to be a known constant.

To intercept hypersonic vehicles, most of the traditional guidance laws were established based on the proportional navigation guidance (PNG) method. Two modified proportional guidance laws were designed in [6,7]. In [8], the composite guidance and navigation strategy were developed against very high-speed targets. To ensure finite-time convergence of the system states, the concept of terminal sliding mode control (TSMC) was put forward. Based on non-singular TSMC theory, guidance laws against stationary or constant velocity targets at a desired impact angle were proposed in [9]. In [10-12], a finite-time convergent sliding-mode guidance law with terminal impact angle constraints was presented. In [13], a guidance law based on fast non-singular terminal sliding mode control was proposed. The tracking error converges to zero in finite time. However, the above algorithms cannot be applied to intercepting hypersonic vehicles.

Chattering phenomenon is an urgent problem to be solved in practical engineering; otherwise, it will not only reduce the guidance precision, but also seriously damage the missile actuator. To suppress this phenomenon, a variety of techniques have been proposed, such as the boundary layer method [14], the high order sliding mode control [15-17], and the filtered switching function [18,19]. In [20], a new discrete-time sliding mode control method based on non-smooth control was proposed. This method can avoid the chattering problem and the generation of over-large control action. In [21], a continuous higher-order sliding mode (HOSM) control scheme was given based on the concept of the geometric homogeneity and super-twisting algorithm. In [22], a control algorithm based on the first order sliding mode technique was proposed. Although lots of above mentioned chattering suppression techniques have been proposed, most of the techniques require the knowledge of the uncertainty bounds. To overcome this drawback, slightly different from the existing conditions, an improved SMC with perturbation estimation, characterized by a PID-type sliding surface and adaptive gains, was proposed in [23]. Two new approaches using adaptive SMC (ASMC) were proposed in [24,25]. These new methods can reduce the gain overestimation and simultaneously speed up the system response to the uncertainties. Through introducing an integral adaptation law, the chatter levels of the sliding mode were significantly reduced.

Another typical feature in the intercepting hypersonic vehicle schemes is that there always exists a saturation limit in the dynamic actuator, which can, if not properly handled, largely lead to performance degradation or, even worse, instability of the system. Many researches have been strived to develop guidance laws that explicitly consider input saturation. In [26,27], a sample saturation function has been used, and the saturated guidance laws have been designed. Nevertheless, this is an approximate method that considers separately the input constraints from system stability. An anti-saturation guidance law using the hyperbolic tangent function is proposed in the study. Compared to [26,27], the innovation of our approach is that the system can be ensured asymptotically stable and finite-time stable. Moreover, this approach is achieved and proved by Lyapunov stability theory, and the detailed designing and proving processes are provided in Section 3.3.

This paper is organized as follows. In Section 2, the non-decoupling three-dimensional engagement dynamics are established. In Section 3, three-dimensional head pursuit guidance laws are designed. Simulation results are presented in Section 4. This paper is closed with conclusions in Section 5.

2. **Problem Statement and Preliminaries.** Figure 1 shows the schematic view of the head pursuit guidance engagement, which can be divided into three phases: approach phase, trajectory bending phase and endgame phase. After being launched, the interceptor is guided to approach the target in a head-on trajectory. And then at a predetermined
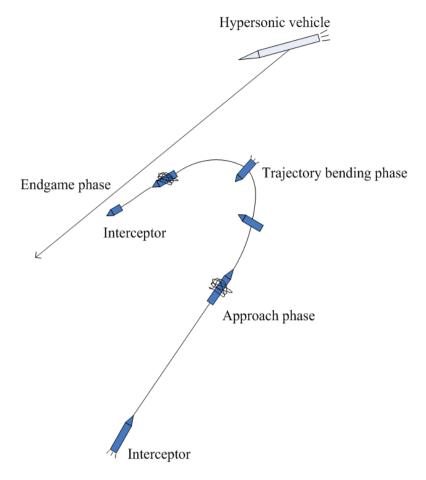
FIGURE 1. Schematic view of a hypersonic vehicle interception engagement

time, the interceptor is steered to bend its flight trajectory until reaching a so-called trajectory matching flight mode. In the beginning of the endgame phase, the interceptor flies ahead of the target at a lower speed and the same general direction as the target. In this unconventional terminal geometry, the target approaches it from the rear end of the interceptor. Using this method, the closing speed is greatly reduced compared to the head-on engagement. The speed requirement for interceptor is significantly lower relative to a traditional tail-chase engagement. The purpose of this paper is to design fast convergence guidance laws using head pursuit guidance method to guide the interceptor to finish the final interception.

In [1], the authors only considered the planar endgame geometry. To be more practical, the three-dimensional engagement geometry is established as Figure 2. In fact, according to this geometry, the performance of the derived guidance law can be enhanced considerably. In the figure, T and M denote the target and missile, respectively. $TX_IY_IZ_I$ is the inertial reference frame. $MX_MY_MZ_M$ is the velocity coordinate system of missile. $TX_TY_TZ_T$ is the velocity coordinate system of target. R is the relative distance between the target and missile. The velocities are denoted by V_t and V_m. a_{ym} and a_{zm} are lateral accelerations of the missile in the yaw and pitch directions, respectively. Similarly, a_{yt} and a_{zt} are the target accelerations. In this geometry, assume that V_m is a constant, which is defined by the angles θ_m and ϕ_m with respect to the line of sight (LOS) frame. θ_t and ϕ_t are the directions of V_t with respect to the LOS frame, respectively. θ_L and ϕ_L represent the directions of LOS with respect to the inertial reference frame. It is assumed that the initial position of the target in the endgame phase is the coordinate origin. The
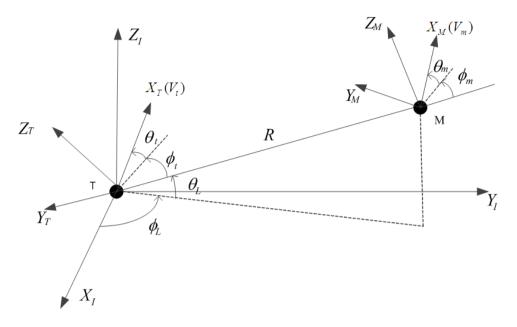
FIGURE 2. Three-dimensional engagement geometry

three-dimensional engagement dynamics can be expressed as follows [28]:

$$\dot{R} = V_m \cos\theta_m \cos\phi_m - V_t \cos\theta_t \cos\phi_t \tag{1}$$

$$R\dot{\theta}_L = V_m \sin\theta_m - V_t \sin\theta_t \tag{2}$$

$$\dot{\phi}_L R \cos\theta_L = V_m \cos\theta_m \sin\phi_m - V_t \cos\theta_t \sin\phi_t \tag{3}$$

$$\dot{\theta}_t = \frac{a_{zt}}{V_t} - \dot{\phi}_L \sin\theta_L \sin\phi_t - \dot{\theta}_L \cos\phi_t \tag{4}$$

$$\dot{\phi}_t = \frac{a_{yt}}{V_t \cos\theta_t} + \dot{\phi}_L \sin\theta_L \cos\phi_t \tan\theta_t - \dot{\theta}_L \sin\phi_t \tan\theta_t - \dot{\phi}_L \cos\theta_L \tag{5}$$

$$\dot{\theta}_m = \frac{a_{zm}}{V_m} - \dot{\phi}_L \sin\theta_L \sin\phi_m - \dot{\theta}_L \cos\phi_m \tag{6}$$

$$\dot{\phi}_m = \frac{a_{ym}}{V_m \cos\theta_m} + \dot{\phi}_L \sin\theta_L \cos\phi_m \tan\theta_m - \dot{\theta}_L \sin\phi_m \tan\theta_m - \dot{\phi}_L \cos\theta_L \tag{7}$$

where lateral accelerations of the missile a_{ym} and a_{zm}, i.e., control inputs, will be designed. Target information including V_t, a_{yt} and a_{zt} is difficult to be accurately measured and is often treated as the external disturbances.

Equation (6) expresses the dynamic of θ_m. Note that the second and third terms contain ϕ_m, i.e., the coupling effect exists between the dynamics Equations (6) and (7). Furthermore, the missile acceleration a_{zm} acts on both θ_m and ϕ_m. Therefore, if a guidance law is designed using two-dimensional decoupled engagement dynamics, the guidance precision and performance must be weakened. Similarly, the dynamic of ϕ_m expressed by Equation (7) is also related to θ_m, and the specific analysis is similar to the above.

According to [1], head pursuit method not only requires that $R = 0$ at the interception point, but also requires that both the target and the interceptor fly in the same direction; hence

$$\lim_{R\to 0}\theta_t = 0, \quad \lim_{R\to 0}\phi_t = 0 \tag{8}$$

$$\lim_{R\to 0}\theta_m = 0, \quad \lim_{R\to 0}\phi_m = 0 \tag{9}$$

In this study, the guidance laws will be designed using the head pursuit to guide the precursor interceptor into the interception point such that Equations (8) and (9) hold simultaneously. Because the interceptor flies in front of the target and is slower than it,

the final geometry can be achieved when the head of the target gets close to the tail of the interceptor. Hence, according to [1], the lead angles of the interceptor are required to be proportional to the target flight direction with regard to the LOS, i.e.,

$$\theta_m = n_1 \theta_t \tag{10}$$

$$\phi_m = n_2 \phi_t \tag{11}$$

where n_i $(i = 1, 2)$ is the guidance constant. According to [1], against a non-maneuvering target, a necessary condition for performing the head pursuit interception is $n_i > {}^{1}\!/\!{}_{K}$ ($K = {}^{V_m}\!/\!{}_{V_t}$). Besides, Equations (10) and (11) can guarantee that θ_m and ϕ_m vanish with θ_t and ϕ_t, respectively.

Lemma 2.1. [1] *During the guidance process, if the system denoted by (1)-(7) satisfies Equations (10) and (11), the target can be successfully intercepted.*

To facilitate the design of guidance laws, the dynamic systems (4)-(7) can be rearranged as Equations (12) and (13).

$$\dot{\boldsymbol{x}} = \boldsymbol{B}\boldsymbol{U} + \boldsymbol{F} \tag{12}$$

$$\dot{\boldsymbol{y}} = \boldsymbol{M} + \boldsymbol{E} \tag{13}$$

$$\boldsymbol{x} = \begin{bmatrix} \theta_m \\ \phi_m \end{bmatrix}, \quad \boldsymbol{y} = \begin{bmatrix} \theta_t \\ \phi_t \end{bmatrix}, \quad \boldsymbol{B} = \begin{bmatrix} \dfrac{1}{V_m} & 0 \\ 0 & \dfrac{1}{V_m \cos\theta_m} \end{bmatrix}$$

$$\boldsymbol{F} = \begin{bmatrix} -\dot{\phi}_L \sin\theta_L \sin\phi_m - \dot{\theta}_L \cos\phi_m \\ \dot{\phi}_L \sin\theta_L \cos\phi_m \tan\theta_m - \dot{\theta}_L \sin\phi_m \tan\theta_m - \dot{\phi}_L \cos\theta_L \end{bmatrix}$$

$$\boldsymbol{M} = \begin{bmatrix} \dfrac{a_{zt}}{V_t} \\ \dfrac{a_{yt}}{V_t \cos\theta_t} \end{bmatrix} = \begin{bmatrix} \dfrac{1}{V_t} & 0 \\ 0 & \dfrac{1}{V_t \cos\theta_t} \end{bmatrix} \begin{bmatrix} a_{zt} \\ a_{yt} \end{bmatrix} = \begin{bmatrix} c_1 & 0 \\ 0 & c_2 \end{bmatrix} \boldsymbol{a} = \boldsymbol{C}\boldsymbol{a}$$

$$\boldsymbol{E} = \begin{bmatrix} -\dot{\phi}_L \sin\theta_L \sin\phi_t - \dot{\theta}_L \cos\phi_t \\ \dot{\phi}_L \sin\theta_L \cos\phi_t \tan\theta_t - \dot{\theta}_L \sin\phi_t \tan\theta_t - \dot{\phi}_L \cos\theta_L \end{bmatrix}$$

where $\boldsymbol{U} \in \boldsymbol{R}^2$ is the input signal, and $\boldsymbol{U} = \begin{bmatrix} u_1 \\ u_2 \end{bmatrix} = \begin{bmatrix} a_{zm} \\ a_{ym} \end{bmatrix}$. $\boldsymbol{M} \in \boldsymbol{R}^2$ is the bounded perturbation.

In Equation (12), since $\boldsymbol{U}$ is multiplied by matrix $\boldsymbol{B}$, a guidance law can be derived only if the matrix $\boldsymbol{B}$ is nonsingular, i.e., $\theta_m \neq \pm(\pi/2)$. Moreover, in the study, it is assumed that the signals including R, $\dot{R}$, θ_L, ϕ_L, $\dot{\theta}_L$, $\dot{\phi}_L$, θ_m, ϕ_m, V_m, θ_t and ϕ_t are measurable. To intercept hypersonic vehicles using head pursuit method, the main purpose of this paper is to design guidance laws such that the systems (1)-(7) satisfy Equations (10) and (11) in finite time. The main results will be given in the section below.

3. Design of Guidance Laws.

3.1. Basic knowledge.
The main objective of this study is to design guidance laws so that the convergence of the systems (1)-(7) to the conditions (10) and (11) can be achieved in finite time. To facilitate the design, the following lemmas are particularized for applications.

Lemma 3.1. [29] *Consider the nonlinear system* $\dot{x} = f(x, t)$, $x \in R^n$. *If there exists a continuous and positive definite function* $V(x)$, *such that*

$$\dot{V}(x) \leq -\mu V(x) - \lambda V^\alpha(x) \tag{14}$$

where μ, λ *and* α *are all constants, and* $\mu, \lambda > 0$ *and* $0 < \alpha < 1$, $x(t_0) = x_0$, *and* t_0 *is the initial time, then the time of system states arriving at the equilibrium point, i.e.,* T, *satisfies the following inequality.*

$$T \leq \frac{1}{\mu(1-\alpha)} \ln \frac{\mu V^{1-\alpha}(x_0) + \lambda}{\lambda} \tag{15}$$

That is, system states are finite-time convergent.

Lemma 3.2. [30] *Consider the nonlinear system* $\dot{x} = f(x, t)$, $x \in R^n$. *If there exists a continuous and positive definite function* $V(x)$, *such that*

$$\dot{V}(x) \leq -\tau \tag{16}$$

where $\tau > 0$ *is a constant, and* t_0 *is the initial time, then the time of system states arriving at the equilibrium point, i.e.,* t^*, *satisfies the following inequality.*

$$t^* = t_0 + \frac{V(t_0)}{\tau} \tag{17}$$

That is, the system states are asymptotically stable and finite-time stable.

3.2. **A novel reaching law.** The discontinuity of guidance laws will cause the chattering phenomenon, which becomes even more serious against hypersonic vehicles. To alleviate this problem, the right reaching law is urgent to be proposed. In conventional reaching laws, constant reaching law has a slow convergence rate and large chattering [31]. Exponent reaching law presents large chattering in the faster convergence rate because of the existing constant term [32]. Power reaching law is smooth when it arrives at the sliding mode surface while it has shortcomings in fast convergence [33].

In the 1980s, Gao [34] put forward the concept of reaching law and designed the power reaching law.

$$\dot{s} = -h \, |s|^\alpha \, \text{sign}(s) \tag{18}$$

where $r_0 > 0$, $r_1 > 0$, and $p > 0$.

The exponent reaching law was proposed in [35] and its function can be expressed as:

$$\dot{s} = -h\text{sign}(s) - ks \tag{19}$$

where $h > 0$, $k > 0$. Note that the application of $-ks$ leads to an increase in convergence time, but $-h\text{sign}(s)$ would result in large chattering.

To avoid the defects of the exponent reaching law and simultaneously keep its advantages, a new reaching law is developed by combining an integral adaptation term with an exponential term.

$$\dot{s} = -ks - (\alpha y + N(s))\text{sign}(s) \tag{20}$$

$$\dot{y} = \alpha|s|, \quad y(0) > 0$$

$$N(S) = r_0 \left(e^{r_1 |s|^p} - r_2 \right)$$

where $k > 0$, $\alpha > 0$, $r_0 > 0$, $r_1 > 0$, $p > 0$, $1 > r_2 > 0$. $-(\alpha y + N(s))\text{sign}(s)$ can reduce chattering and $-ks$ can accelerate convergence.

3.3. **Design of guidance laws.** Equation (21) is chosen as the sliding mode manifold surface.

$$\boldsymbol{S} = \begin{bmatrix} s_1 \\ s_2 \end{bmatrix} = \begin{bmatrix} \theta_m - n_1\theta_t \\ \phi_m - n_2\phi_t \end{bmatrix} \tag{21}$$

Then, the derivative of $\boldsymbol{S}$ can be expressed as Equation (22).

$$\dot{\boldsymbol{S}} = \begin{bmatrix} \dot{s}_1 \\ \dot{s}_2 \end{bmatrix} = \dot{\boldsymbol{x}} - \boldsymbol{n}\dot{\boldsymbol{y}} = \boldsymbol{BU} + \boldsymbol{F} - \boldsymbol{n}(\boldsymbol{M} + \boldsymbol{E}) \tag{22}$$

where $\boldsymbol{n} = \begin{bmatrix} n_1 & 0 \\ 0 & n_2 \end{bmatrix}$.

In this study, the new reaching law, i.e., Equation (20), is adopted. Specifically, the form can be expressed as follows:

$$\dot{\boldsymbol{S}} = -\boldsymbol{kS} - \boldsymbol{Q}(\alpha\boldsymbol{y} + \boldsymbol{N}(\boldsymbol{S})) \tag{23}$$

$$\dot{\boldsymbol{y}} = \begin{bmatrix} \dot{y}_1 \\ \dot{y}_2 \end{bmatrix} = \begin{bmatrix} \alpha\,|s_1| \\ \alpha\,|s_2| \end{bmatrix}, \quad y_i(0) > 0, \quad \boldsymbol{Q} = \begin{bmatrix} \text{sign}(s_1) & 0 \\ 0 & \text{sign}(s_1) \end{bmatrix},$$

$$\boldsymbol{N}(\boldsymbol{S}) = \begin{bmatrix} r_0\left(e^{r_1|s_1|^p} - r_2\right) \\ r_0\left(e^{r_1|s_2|^p} - r_2\right) \end{bmatrix}$$

Substituting Equation (23) into Equation (22), a new finite-time adaptive guidance law against hypersonic vehicles is established as follows:

$$\boldsymbol{U}_1 = -\boldsymbol{B}^{-1}\left(\boldsymbol{F} - \boldsymbol{nE} + \boldsymbol{kS} + \boldsymbol{Q}(\alpha\boldsymbol{y} + \boldsymbol{N}(\boldsymbol{S}))\right) \tag{24}$$

where $\boldsymbol{k} = \begin{bmatrix} k_1 & 0 \\ 0 & k_2 \end{bmatrix}$, $(k_1, k_2 > 0)$, $k = \min(k_1, k_2)$, and $\alpha > \max(n_1, n_2)$.

Theorem 3.1. *Consider the systems (1)-(7) Suppose that the external disturbance $\boldsymbol{M}$ is bounded. If the guidance law is designed as Equation (24), the sliding mode surface (21) can converge to zero in finite time.*

Proof: Assuming that $|m_1| \leq \varepsilon_1$ and $|m_2| \leq \varepsilon_2$, $\varepsilon = \begin{bmatrix} \varepsilon_1 \\ \varepsilon_2 \end{bmatrix}$. Consider the Lyapunov function candidate as Equation (25)

$$V_1 = \frac{1}{2}\boldsymbol{S}^{\mathrm{T}}\boldsymbol{S} + \frac{1}{2}(\boldsymbol{\varepsilon} - \boldsymbol{y})^{\mathrm{T}}(\boldsymbol{\varepsilon} - \boldsymbol{y}) \tag{25}$$

The time derivative of the Lyapunov function V_1 along with Equations (1)-(7) results in

$$\begin{aligned}
\dot{V}_1 &= \boldsymbol{S}^{\mathrm{T}}\dot{\boldsymbol{S}} - (\boldsymbol{\varepsilon} - \boldsymbol{y}(\boldsymbol{S}))^{\mathrm{T}}\dot{\boldsymbol{y}}(\boldsymbol{S}) \\
&= \boldsymbol{S}^{\mathrm{T}}(\boldsymbol{BU} + \boldsymbol{F} - \boldsymbol{n}(\boldsymbol{M} + \boldsymbol{E})) - (\boldsymbol{\varepsilon} - \boldsymbol{y})^{\mathrm{T}}\begin{bmatrix} \alpha\,|s_1| & 0 \\ 0 & \alpha\,|s_2| \end{bmatrix} \\
&= \boldsymbol{S}^{\mathrm{T}}(-\boldsymbol{nM} - \boldsymbol{kS} - (\alpha\boldsymbol{y} + \boldsymbol{N}(\boldsymbol{S}))\text{sign}(\boldsymbol{S})) - (\boldsymbol{\varepsilon} - \boldsymbol{y})^{\mathrm{T}}\begin{bmatrix} \alpha\,|s_1| & 0 \\ 0 & \alpha\,|s_2| \end{bmatrix} \\
&\leq -k\boldsymbol{S}^{\mathrm{T}}\boldsymbol{S} + \sum_{i=1}^{2}|s_i|\,n_i\varepsilon_i - \boldsymbol{S}^{\mathrm{T}}\boldsymbol{N}(\boldsymbol{S})\text{sign}(\boldsymbol{S}) - \sum_{i=1}^{2}|s_i|\,\alpha\varepsilon_i \\
&= -k\boldsymbol{S}^{\mathrm{T}}\boldsymbol{S} - \boldsymbol{S}^{\mathrm{T}}\boldsymbol{N}(\boldsymbol{S})\text{sign}(\boldsymbol{S}) - \sum_{i=1}^{2}|s_i|\,\varepsilon_i(\alpha - n_i) \\
&\leq 0
\end{aligned}$$

From the above inequality, we have $V_1(t) \leq V_1(0)$, which implies that $V_1(t)$ is bounded. Hence, it can be concluded that s_j and $\varepsilon_i - y_i$ $(i = 1, 2)$ are all bounded.

In addition, consider another Lyapunov function as Equation (26).

$$V_2 = \frac{1}{2}\boldsymbol{S}^{\mathrm{T}}\boldsymbol{S} \tag{26}$$

The time derivative of the Lyapunov function V_2 can be expressed as:

$$
\begin{aligned}
\dot{V}_2 &= \boldsymbol{S}^{\mathrm{T}}\dot{\boldsymbol{S}} \\
&= \boldsymbol{S}^{\mathrm{T}}(-\boldsymbol{n}\boldsymbol{M} - \boldsymbol{k}\boldsymbol{S} - (\alpha\boldsymbol{y} + \boldsymbol{N}(\boldsymbol{S}))\mathrm{sign}(\boldsymbol{S})) \\
&\leq -k\boldsymbol{S}^{\mathrm{T}}\boldsymbol{S} + \sum_{i=1}^{2}|s_i|\,n_i\varepsilon_i - \boldsymbol{S}^{\mathrm{T}}\boldsymbol{N}(\boldsymbol{S})\mathrm{sign}(\boldsymbol{S}) - \sum_{i=1}^{2}|s_i|\,\alpha y_i \\
&= -k\boldsymbol{S}^{\mathrm{T}}\boldsymbol{S} - \boldsymbol{S}^{\mathrm{T}}\boldsymbol{N}(\boldsymbol{S})\mathrm{sign}(\boldsymbol{S}) - \sum_{i=1}^{2}|s_i|\,(\alpha y_i - \varepsilon_i n_i)
\end{aligned}
$$

Because $y_i(0) > 0$, and $\dot{y}_i = \alpha\,|s_i| \geq 0$, we obtain that $y_i(t) > y_i(0)$. Choose $y_i(0)$ large enough, and α satisfies $\alpha \geq \frac{n_i\sqrt{s_i^2(0)+y_i^2(0)}}{y_i(0)} + n_i$. Then, it can be obtained that

$$
\begin{aligned}
n_i\varepsilon_i - \alpha y_i &\leq n_i\varepsilon_i - n_i\sqrt{s_i^2(0) + y_i^2(0)} - n_i y_i(0) \\
&\leq n_i(\varepsilon_i - y_i(0)) - n_i\sqrt{s_i^2(0) + y_i^2(0)} \\
&\leq n_i\,|\varepsilon_i - y_i(0)| - n_i\sqrt{s_i^2(0) + y_i^2(0)} \\
&\leq n_i\sqrt{y_i^2(0)} - n_i\sqrt{s_i^2(0) + y_i^2(0)} \\
&\leq 0
\end{aligned}
\tag{27}
$$

Combining Equation (27), $\dot{V}_2$ continues to be derived as follows.

$$
\begin{aligned}
\dot{V}_2 &\leq -k\boldsymbol{S}^{\mathrm{T}}\boldsymbol{S} - \boldsymbol{S}^{\mathrm{T}}\boldsymbol{N}(\boldsymbol{S})\mathrm{sign}(\boldsymbol{S}) - \sum_{i=1}^{2}|s_i|\,(\alpha y_i - \varepsilon_i n_i) \\
&\leq -k\boldsymbol{S}^{\mathrm{T}}\boldsymbol{S} - \boldsymbol{S}^{\mathrm{T}}\boldsymbol{N}(\boldsymbol{S})\mathrm{sign}(\boldsymbol{S}) \\
&\leq -2kV_2 - \sqrt{2}\min\left(r_0\left(e^{r_1|s_1|^p} - r_2\right), r_0\left(e^{r_1|s_2|^p} - r_2\right)\right)V_2^{\frac{1}{2}}
\end{aligned}
\tag{28}
$$

According to Lemma 3.1, Equation (28) indicates that the finite-time convergence of the sliding mode surface is available. That is to say, the head pursuit conditions (10) and (11) can be obtained within finite time. The proof of Theorem 3.1 is completed.

Remark 3.1. *In guidance law (24), the role of the term $\boldsymbol{y}$ is to compensate for external uncertainties with unknown bounds and forces the finite-time convergence of the sliding variables to the sliding surface. However, in the initial stage, the numerical value of $\boldsymbol{y}$ is very small, which will result in a long convergence time. To make up for this defect, the exponential term $\boldsymbol{N}(\boldsymbol{S})$ is added, which provides an extra but sufficiently high gain when the state is far away from the sliding surface. In this way, convergence speed can be accelerated and the response of the system to the external perturbations is also speeded up. When $\boldsymbol{S} \to \boldsymbol{0}$, $\boldsymbol{y}$ gradually slows down until it stops growing. Moreover, $\boldsymbol{N}(\boldsymbol{S})$ reduces its value rapidly until it disappears at the sliding surface. On reaching the sliding surface, the overall gain can be reduced, i.e., this method can reduce the unwanted chattering level.*

In Theorem 3.1, a new finite-time adaptive guidance law against hypersonic vehicles is proposed. However, the capacity of dynamic actuators is limited in practice. Therefore, input constraints should be taken into account. The finite-time guidance law with anti-saturation characteristic is designed in this section using the hyperbolic tangent function and auxiliary system.

$$\boldsymbol{U}_2 = -a_1 \tanh(\varepsilon_1 \boldsymbol{\zeta}) - a_2 \tanh(\varepsilon_2 \boldsymbol{S}) \tag{29}$$

$$\boldsymbol{\gamma} = \boldsymbol{S} - \boldsymbol{\zeta}$$

$$\dot{\boldsymbol{\zeta}} = \boldsymbol{B}\boldsymbol{U}_2 + \boldsymbol{F} - \boldsymbol{n}\boldsymbol{E} + \left[\boldsymbol{S}^{\mathrm{T}}(\boldsymbol{B}\boldsymbol{U}_2 + \boldsymbol{F} - \boldsymbol{n}\boldsymbol{E})\right] \frac{\boldsymbol{\gamma}}{\boldsymbol{\gamma}^{\mathrm{T}}\boldsymbol{\gamma}} + a_3\boldsymbol{\gamma} + \left(a_4 + m \left\|\boldsymbol{S}^{\mathrm{T}}\boldsymbol{n}\right\|\right) \frac{\boldsymbol{\gamma}}{\boldsymbol{\gamma}^{\mathrm{T}}\boldsymbol{\gamma}} + a_5 \mathrm{sign}(\boldsymbol{\gamma})$$

where a_1, a_2, a_3, a_4, ε_1 and ε_2 are positive constants. $n = \max(n_1, n_2)$, $a_5 > nm$.

Theorem 3.2. *Consider the systems (1)-(7). Suppose that the external disturbance $\|\boldsymbol{M}\|$ is bounded, and $\|\boldsymbol{M}\| \leq m$. If the guidance law is designed as Equation (29), the sliding mode surface (21) can converge to zero with asymptotical stability and finite-time stability.*

Proof: Consider the Lyapunov function candidate as Equation (30).

$$V_3 = \frac{1}{2}\boldsymbol{\gamma}^{\mathrm{T}}\boldsymbol{\gamma} + \frac{1}{2}\boldsymbol{S}^{\mathrm{T}}\boldsymbol{S} \tag{30}$$

The time derivative of the Lyapunov function V_3 along with Equations (1)-(7) results in:

$$
\begin{aligned}
\dot{V}_3 &= \boldsymbol{\gamma}^{\mathrm{T}}\dot{\boldsymbol{\gamma}} + \boldsymbol{S}^{\mathrm{T}}\dot{\boldsymbol{S}} \\
&= \boldsymbol{\gamma}^{\mathrm{T}}\left(\boldsymbol{B}\boldsymbol{U} + \boldsymbol{F} - \boldsymbol{n}(\boldsymbol{M} + \boldsymbol{E}) - \dot{\boldsymbol{\zeta}}\right) + \boldsymbol{S}^{\mathrm{T}}(\boldsymbol{B}\boldsymbol{U} + \boldsymbol{F} - \boldsymbol{n}(\boldsymbol{M} + \boldsymbol{E})) \\
&= -\boldsymbol{\gamma}^{\mathrm{T}}\boldsymbol{n}\boldsymbol{M} - \boldsymbol{S}^{\mathrm{T}}\boldsymbol{n}\boldsymbol{M} - \boldsymbol{\gamma}^{\mathrm{T}}\left(a_3\boldsymbol{\gamma} + \left(a_4 + m\left\|\boldsymbol{S}^{\mathrm{T}}\boldsymbol{n}\right\|\right)\frac{\boldsymbol{\gamma}}{\boldsymbol{\gamma}^{\mathrm{T}}\boldsymbol{\gamma}} + a_5\mathrm{sign}(\boldsymbol{\gamma})\right) \\
&\leq \|\boldsymbol{\gamma}\|\,\|\boldsymbol{n}\boldsymbol{M}\| + m\left\|\boldsymbol{S}^{\mathrm{T}}\boldsymbol{n}\right\| - m\left\|\boldsymbol{S}^{\mathrm{T}}\boldsymbol{n}\right\| - a_5\|\boldsymbol{\gamma}\| - \boldsymbol{\gamma}^{\mathrm{T}}\left(a_3\boldsymbol{\gamma} + a_4\frac{\boldsymbol{\gamma}}{\boldsymbol{\gamma}^{\mathrm{T}}\boldsymbol{\gamma}}\right) \\
&\leq nm\|\boldsymbol{\gamma}\| + m\left\|\boldsymbol{S}^{\mathrm{T}}\boldsymbol{n}\right\| - m\left\|\boldsymbol{S}^{\mathrm{T}}\boldsymbol{n}\right\| - a_5\|\boldsymbol{\gamma}\| - \boldsymbol{\gamma}^{\mathrm{T}}\left(a_3\boldsymbol{\gamma} + a_4\frac{\boldsymbol{\gamma}}{\boldsymbol{\gamma}^{\mathrm{T}}\boldsymbol{\gamma}}\right) \\
&= -\|\boldsymbol{\gamma}\|\,(a_5 - \|\boldsymbol{n}\boldsymbol{M}\|) - \boldsymbol{\gamma}^{\mathrm{T}}\left(a_3\boldsymbol{\gamma} + a_4\frac{\boldsymbol{\gamma}}{\boldsymbol{\gamma}^{\mathrm{T}}\boldsymbol{\gamma}}\right) \\
&\leq -\boldsymbol{\gamma}^{\mathrm{T}}\left(a_3\boldsymbol{\gamma} + a_4\frac{\boldsymbol{\gamma}}{\boldsymbol{\gamma}^{\mathrm{T}}\boldsymbol{\gamma}}\right) \\
&\leq -a_4
\end{aligned}
$$

According to Lemma 3.2, the sliding mode $\boldsymbol{S}$ converges to $\boldsymbol{0}$ with asymptotical stability and finite-time stability. So the conclusions of Theorem 3.2 are easily obtained.

Remark 3.2. *Based on the above analysis, our approach is novel in which the sliding mode surface converging to the origin is asymptotically stable and finite-time stable, and can be achieved and proved in theory.*

4. **Simulation Results.** In this section, numerical simulations are implemented to illustrate the performance of the proposed guidance laws. Each of the following subsections is divided into two parts to carry out simulations. The first part is to verify the effectiveness of the guidance law. The second part is to verify the superiority of the designed guidance laws by comparing with traditional guidance laws.
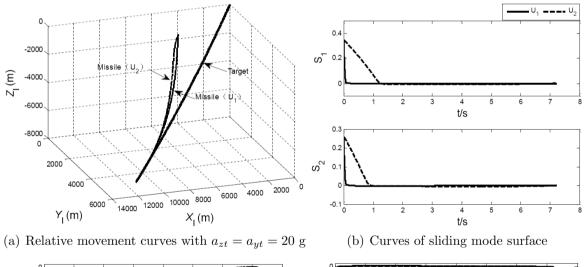
4.1. **Effectiveness verification.** In order to demonstrate the effectiveness of guidance law U_1, we consider the following three target maneuvers:

Case 1: $a_{zt} = a_{yt} = 19.6$ m/s^2;

Case 2: $a_{zt} = a_{yt} = 19.6\cos(2t)$ m/s^2;

Case 3: a_{zt} and a_{yt} are step signals with an amplitude of 19.6 m/s^2 at $t = 4$ s.

The initial engagement parameters are listed in Table 1 [1,5].

TABLE 1. The initial conditions for the missile and target

Initial condition	Dataset 1
$R(0)$	5000 m
$\theta_L(0)$	−10 deg
$\phi_L(0)$	−12 deg
$\theta_m(0)$	−20 deg
$\phi_m(0)$	−15 deg
V_m	1600 m/s
$\theta_t(0)$	−20 deg
$\phi_t(0)$	−15 deg
V_t	2100 m/s

(a) Relative movement curves with $a_{zt} = a_{yt} = 20$ g

(b) Curves of sliding mode surface

(c) Curves of θ_m, θ_t, ϕ_m and ϕ_t
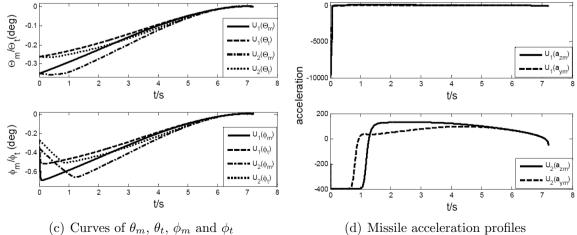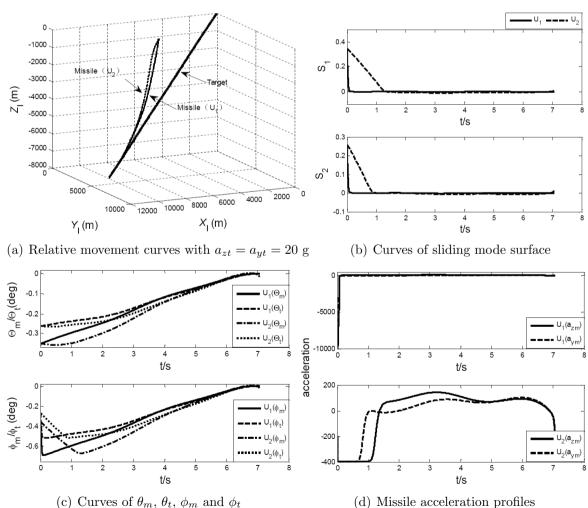
(d) Missile acceleration profiles

FIGURE 3. Simulation results when $a_{zt} = a_{yt} = 20$ g

The parameters of $\boldsymbol{U}_1$ are chosen as $\boldsymbol{k} = \begin{bmatrix} 10 & 0 \\ 0 & 10 \end{bmatrix}$, $\boldsymbol{n} = \begin{bmatrix} 2 & 0 \\ 0 & 2 \end{bmatrix}$, $\alpha = 16$, $r_2 = 0.97$, $\beta = 5$, $r_0 = 5$, $r_1 = 1$, $p = 1$. The parameters of $\boldsymbol{U}_2$ are chosen as $\boldsymbol{n} = \begin{bmatrix} 2 & 0 \\ 0 & 2 \end{bmatrix}$, $a_1 = 200$, $a_2 = 200$, $a_3 = 0.01$, $a_4 = 2$, $a_5 = 2$, $\varepsilon_1 = 40$ and $\varepsilon_2 = 40$.

Case 1: Figure 3 shows the simulation results of guidance laws designed in this paper, i.e., $\boldsymbol{U}_1$ and $\boldsymbol{U}_2$. Figure 3(a) presents relative movement curves with Case 1. It can be obtained that both of $\boldsymbol{U}_1$ and $\boldsymbol{U}_2$ ensure that the missile successfully intercepts the target. Figure 3(b) shows the curves of sliding mode surface. From it, we can obtain that the convergence speed under $\boldsymbol{U}_1$ is much faster than it under $\boldsymbol{U}_2$. It also illustrates that the convergence rate can be accelerated without overloading limit. Figure 3(c) shows the curves of θ_m, θ_t, ϕ_m, and ϕ_t, and it verifies that θ_m becomes 2 times of θ_t within a finite time, and finally converges to zero. Similarly, ϕ_m becomes 2 times of ϕ_t. Figure 3(d) presents missile acceleration profiles. Note that, in the initial stage of guidance process, the value of $\boldsymbol{U}_1$ reaches about -1000 g; however, it cannot be satisfied in practice. Although there is a saturation phenomenon in $\boldsymbol{U}_2$, it is within a reasonable range.

Case 2: With the same initial conditions and parameters, Case 2 is also simulated. Figure 4 shows the simulation results of guidance laws designed in this paper, i.e., $\boldsymbol{U}_1$ and $\boldsymbol{U}_2$. Figure 4(a) presents relative movement curves with Case 2. Both of $\boldsymbol{U}_1$ and $\boldsymbol{U}_2$ can

(a) Relative movement curves with $a_{zt} = a_{yt} = 20$ g

(b) Curves of sliding mode surface

(c) Curves of θ_m, θ_t, ϕ_m and ϕ_t

(d) Missile acceleration profiles

FIGURE 4. Simulation results when $a_{zt} = a_{yt} = 20$ g

(a) Relative movement curves with $a_{zt} = a_{yt} = 20$ g

(b) Curves of sliding mode surface

(c) Curves of θ_m, θ_t, ϕ_m and ϕ_t
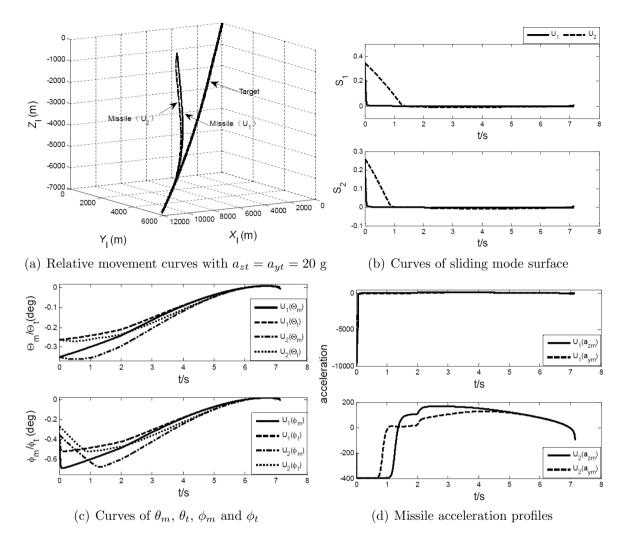
(d) Missile acceleration profiles

FIGURE 5. Simulation results when $a_{zt} = a_{yt} = 20$ g

still ensure that the interception mission is completed successfully. Figure 4(b) shows the curves of sliding mode surface. Figure 4(c) shows the curves of θ_m, θ_t, ϕ_m, and ϕ_t. Figure 4(d) presents missile acceleration profiles. Figure 4 shows the same situation as Figure 3, so no longer repeated here.

Case 3: With the same initial conditions and parameters, Case 3 is also simulated. Figure 5 shows the simulation results of guidance laws designed in this paper. Figure 5(a) presents relative movement curves with Case 3. Both of U_1 and U_2 can still ensure that the missile successfully intercepts the target. Figure 5(b) shows the curves of sliding mode surface. Figure 5(c) shows the curves of θ_m, θ_t, ϕ_m, and ϕ_t. Figure 5(d) presents missile acceleration profiles. Figure 5 presents the same situation as Figure 3, so no longer repeated here. To sum up, U_1 and U_2 can ensure the successful intercept of a hypersonic vehicle with three different maneuvering scenarios. It also proves the validity of guidance laws designed in this study.

Table 2 presents the interception time and miss distance with three different cases. It can be obtained that the interception time is different with different cases, but the miss distances are all within a reasonable range under both U_1 and U_2. Therefore, the effectiveness of the designed guidance laws is further proved.

4.2. **Superiority verification.** To further prove the superiority of the proposed continuous adaptive sliding mode guidance law U_1 in chattering elimination, the sliding mode
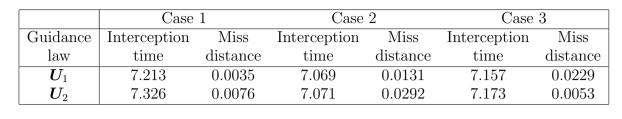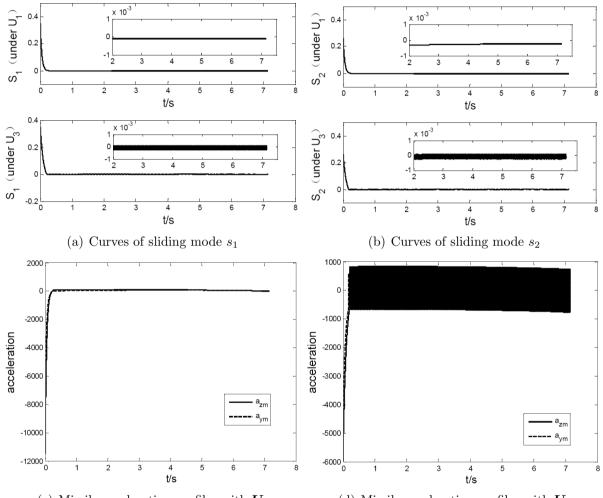
TABLE 2. Interception time and miss distance

Guidance law	Case 1		Case 2		Case 3	
	Interception time	Miss distance	Interception time	Miss distance	Interception time	Miss distance
U_1	7.213	0.0035	7.069	0.0131	7.157	0.0229
U_2	7.326	0.0076	7.071	0.0292	7.173	0.0053

(a) Curves of sliding mode s_1

(b) Curves of sliding mode s_2

(c) Missile acceleration profiles with U_1

(d) Missile acceleration profiles with U_3

FIGURE 6. Comparison between U_1 and U_3 with $a_{zt} = a_{yt} = 20$ g

guidance law U_3 is chosen to compare with it. The guidance law U_3 is established by the application of the exponent reaching law (19).

$$U_3 = -B^{-1}(F - nE + kS + h\text{sign}(S)) \tag{31}$$

where $h > 0$ and $h = 0.2$. To ensure fair and valid comparisons, the other parameters of U_3 are selected as the same as those of U_1. In this section, the target acceleration is selected as 2 g.

Figure 6 shows the comparison results between U_1 and U_3 including the curves of sliding mode surface and missile acceleration. We can obtain that the sliding mode surfaces and missile acceleration profiles have serious chattering phenomenon under U_3; however, the

undesired chattering is reduced effectively by guidance law $\boldsymbol{U}_1$. Therefore, the good performance and superiority of the guidance law $\boldsymbol{U}_1$ have been sufficiently demonstrated.

5. **Conclusions.** In this paper, two three-dimensional head pursuit adaptive sliding mode guidance laws have been presented. The system can be ensured to converge to the head pursuit guidance conditions in finite time. The first guidance law can deal with the unknown upper bound of the external disturbances. The second guidance law guarantees that the sliding surface is asymptotically stable and finite-time stable with input saturation. However, the second guidance law cannot deal with the external perturbation. How to derive the anti-saturation guidance law that can deal with the external perturbation is still a challenging problem, which is also the next research direction of this paper.

REFERENCES

[1] O. M. Golan and T. Shima, Head pursuit guidance for hypervelocity interception, *Proc. of the AIAA Conf. on Guidance, Navigation, and Control Conference and Exhibit*, Providence, Rhode Island, pp.16-19, 2004.

[2] O. M. Golan and T. Shima, Precursor interceptor guidance using the sliding mode approach, *Proc. of the AIAA Conf. on Guidance, Navigation, and Control Conference and Exhibit*, San Francisco, CA, pp.15-18, 2005.

[3] O. M. Golan and T. Shima, Head pursuit guidance, *Journal of Guidance, Control, and Dynamics*, vol.30, no.5, pp.1437-1444, 2007.

[4] Y. A. Zhang, H. L. Wu, Y. Liang and J. P. Zhang, Three-dimensional head pursuit guidance law considering dynamic characteristics of uncertain hybrid control system, *Systems Engineering and Electronics*, vol.37, no.6, pp.1354-1361, 2015.

[5] L. Z. Ge, Y. Shen, Y. F. Gao and L. J. Zhao, Head pursuit variable structure guidance law for three-dimensional space interception, *Chinese Journal of Aeronautics*, vol.21, no.3, pp.247-251, 2008.

[6] T. Kuroda and F. Imado, Advanced missile guidance system against a very high speed maneuvering target, *Proc. of the AIAA Conf. on Guidance, Navigation, and Control Conference*, pp.176-180, 1989.

[7] T. Kuroda and F. Imado, Advanced missile guidance system against very high speed maneuvering target, *Proc. of the AIAA Conf. on Guidance, Navigation, and Control Conference*, pp.320-324, 1988.

[8] D. R. Taur, Composite guidance and navigation strategy for a SAM against high-speed target, *Proc. of AIAA Conf. on Guidance, Navigation, and Control Conference and Exhibit*, Austin, TX, pp.1-5, 2003.

[9] S. R. Kumar, S. Rao and D. Ghose, Non-singular terminal sliding mode guidance and control with terminal angle constraints for non-maneuvering targets, *Proc. of IEEE the 12th Workshop on Variable Structure Systems*, Mumbai, pp.291-296, 2012.

[10] S. R. Kumar, S. Rao and D. Ghose, Nonsingular terminal sliding mode guidance with impact angle constraints, *Journal of Guidance, Control, and Dynamics*, vol.37, no.4, pp.1114-1130, 2014.

[11] S. Xiong, W. Wang and X. Liu, Guidance law against maneuvering targets with intercept angle constraint, *ISA Transactions*, vol.53, no.4, pp.1332-1342, 2014.

[12] S. He and D. Lin, Sliding mode-based continuous guidance law with terminal angle constraint, *The Aeronautical Journal*, vol.120, no.1229, pp.1175-1195, 2016.

[13] J. Song, S. M. Song and H. B. Zhou, Adaptive nonsingular fast terminal sliding mode guidance law with impact angle constraints, *International Journal of Control, Automation and Systems*, vol.14, no.1, pp.99-114, 2016.

[14] V. I. Utkin, *Sliding Modes in Control and Optimization*, Springer Science & Business Media, Netherlands, 2013.

[15] A. Levant, Principles of 2-sliding mode design, *Automatica*, vol.43, no.43, pp.576-586, 2007.

[16] P. Li and Z. Q. Zheng, Robust adaptive second-order sliding-mode control with fast transient performance, *IET Control Theory and Applications*, vol.6, no.2, pp.305-312, 2012.

[17] Y. Shtessel, I. Shkolnilov and M. Brown, An asymptotic second-order smooth sliding mode control, *Asian Journal of Control*, vol.5, no.4, pp.498-504, 2003.

[18] H. Lee and V. Utkin, Chattering suppression methods in sliding mode control systems, *Annual Reviews in Control*, vol.31, no.1, pp.179-188, 2007.

[19] V. I. Utkin and A. S. Poznyak, Adaptive sliding mode control with application to super-twist algorithm: Equivalent control method, *Automatica*, vol.1, no.49, pp.39-47, 2013.

[20] H. Du, X. Yu, M. Z. Q. Chen and S. H. Li, Chattering-free discrete-time sliding mode control, *Automatica*, vol.68, pp.87-91, 2016.

[21] Y. Han and X. Liu, Continuous higher-order sliding mode control with time-varying gain for a class of uncertain nonlinear systems, *ISA Transactions*, vol.62, no.2016, pp.193-201, 2016.

[22] R. Rascón, O. Peñaloza-Mejía and J. G. Castro, Improving first order sliding mode control on second order mechanical systems, *European Journal of Control*, vol.29, no.2016, pp.74-80, 2016.

[23] Y. Li and Q. Xu, Adaptive sliding mode control with perturbation estimation and PID sliding surface for motion tracking of a Piezo-driven micromanipulator, *IEEE Trans. Control Systems Technology*, vol.18, no.4, pp.798-810, 2010.

[24] J. Zhu and K. Khayati, Adaptive sliding mode control with smooth switching gain, *Proc of the 27th Conf. on Electrical and Computer Engineering*, Canada, pp.1-6, 2014.

[25] J. Zhu and K. Khayati, A new approach for adaptive sliding mode control: Integral/exponential gain law, *Transactions of the Institute of Measurement and Control*, vol.38, no.4, pp.385-394, 2016.

[26] D. Zhang, P. Shi, Q. G. Wang et al., Analysis and synthesis of networked control systems: A survey of recent advances and challenges, *ISA Transactions*, vol.66, no.2017, pp.376-392, 2017.

[27] K. Ma, H. K. Khalil and Y. Yao, Guidance law implementation with performance recovery using an extended high-gain observer, *Aerospace Science and Technology*, vol.24, no.1, pp.177-186, 2013.

[28] S. H. Song and I. J. Ha, A Lyapunov-like approach to performance analysis of 3-dimensional pure PNG laws, *Aerospace and Electronic Systems*, vol.30, no.1, pp.238-248, 1994.

[29] S. H. Yu, X. H. Yu et al., Continuous finite-time control for robotic manipulators with terminal sliding mode, *Automatica*, vol.41, no.11, pp.1957-1964, 2005.

[30] M. Huo, X. Huo and H. R. Karimi, Finite-time control for attitude tracking maneuver of rigid satellite, *Abstract and Applied Analysis*, vol.2014, no.5, pp.1-15, 2014.

[31] A. Mehta and B. Bandyopadhyay, In frequency shaped and observer-based discrete-time sliding mode control, *IEEE Trans. Control Systems Technology*, vol.37, no.5, p.925, 2015.

[32] W. F. Xie, Sliding-mode-observer-based adaptive control for servo actuator with friction, *IEEE Trans. Industrial Electronics*, vol.54, no.3, pp.1517-1527, 2007.

[33] Y. Niu, D. W. Hu and Z. Wang, Improved sliding mode control for discrete-time systems via reaching law, *IET Control Theory & Applications*, vol.4, no.11, pp.2245-2251, 2010.

[34] W. B. Gao, *Theory and Design Method of Variable Structure Control*, Science Press, Beijing, 1996.

[35] C. J. Fallaha, Sliding-mode robot control with exponential reaching law, *IEEE Trans. Industrial Electronics*, vol.58, no.2, pp.600-610, 2011.